# Study of the decay $B_s^0 \to J/\psi f_2'(1525)$ in $\mu^+\mu^- K^+ K^-$ final states

V. M. Abazov,[32] B. Abbott,[70] B. S. Acharya,[26] M. Adams,[46] T. Adams,[44] G. D. Alexeev,[32] G. Alkhazov,[36] A. Alton,[58,*] G. Alverson,[57] M. Aoki,[45] A. Askew,[44] S. Atkins,[55] K. Augsten,[7] C. Avila,[5] F. Badaud,[10] L. Bagby,[45] B. Baldin,[45] D. V. Bandurin,[44] S. Banerjee,[26] E. Barberis,[57] P. Baringer,[53] J. Barreto,[2] J. F. Bartlett,[45] U. Bassler,[15] V. Bazterra,[46] A. Bean,[53] M. Begalli,[2] L. Bellantoni,[45] S. B. Beri,[24] G. Bernardi,[14] R. Bernhard,[19] I. Bertram,[39] M. Besançon,[15] R. Beuselinck,[40] V. A. Bezzubov,[35] P. C. Bhat,[45] S. Bhatia,[60] V. Bhatnagar,[24] G. Blazey,[47] S. Blessing,[44] K. Bloom,[61] A. Boehnlein,[45] D. Boline,[67] E. E. Boos,[34] G. Borissov,[39] T. Bose,[56] A. Brandt,[73] O. Brandt,[20] R. Brock,[59] G. Brooijmans,[65] A. Bross,[45] D. Brown,[14] J. Brown,[14] X. B. Bu,[45] M. Buehler,[45] V. Buescher,[21] V. Bunichev,[34] S. Burdin,[39,†] C. P. Buszello,[38] E. Camacho-Pérez,[29] B. C. K. Casey,[45] H. Castilla-Valdez,[29] S. Caughron,[59] S. Chakrabarti,[67] D. Chakraborty,[47] K. M. Chan,[51] A. Chandra,[75] E. Chapon,[15] G. Chen,[53] S. Chevalier-Théry,[15] D. K. Cho,[72] S. W. Cho,[28] S. Choi,[28] B. Choudhary,[25] S. Cihangir,[45] D. Claes,[61] J. Clutter,[53] M. Cooke,[45] W. E. Cooper,[45] M. Corcoran,[75] F. Couderc,[15] M.-C. Cousinou,[12] A. Croc,[15] D. Cutts,[72] A. Das,[42] G. Davies,[40] S. J. de Jong,[30,31] E. De La Cruz-Burelo,[29] F. Déliot,[15] R. Demina,[66] D. Denisov,[45] S. P. Denisov,[35] S. Desai,[45] C. Deterre,[15] K. DeVaughan,[61] H. T. Diehl,[45] M. Diesburg,[45] P. F. Ding,[41] A. Dominguez,[61] A. Dubey,[25] L. V. Dudko,[34] D. Duggan,[62] A. Duperrin,[12] S. Dutt,[24] A. Dyshkant,[47] M. Eads,[61] D. Edmunds,[59] J. Ellison,[43] V. D. Elvira,[45] Y. Enari,[14] H. Evans,[49] A. Evdokimov,[68] V. N. Evdokimov,[35] G. Facini,[57] L. Feng,[47] T. Ferbel,[66] F. Fiedler,[21] F. Filthaut,[30,31] W. Fisher,[59] H. E. Fisk,[45] M. Fortner,[47] H. Fox,[39] S. Fuess,[45] A. Garcia-Bellido,[66] J. A. García-González,[29] G. A. García-Guerra,[29,‡] V. Gavrilov,[33] P. Gay,[10] W. Geng,[12,59] D. Gerbaudo,[63] C. E. Gerber,[46] Y. Gershtein,[62] G. Ginther,[45,66] G. Golovanov,[32] A. Goussiou,[77] P. D. Grannis,[67] S. Greder,[16] H. Greenlee,[45] G. Grenier,[17] Ph. Gris,[10] J.-F. Grivaz,[13] A. Grohsjean,[15,§] S. Grünendahl,[45] M. W. Grünewald,[27] T. Guillemin,[13] G. Gutierrez,[45] P. Gutierrez,[70] A. Haas,[65,‖] S. Hagopian,[44] J. Haley,[57] L. Han,[4] K. Harder,[41] A. Harel,[66] J. M. Hauptman,[52] J. Hays,[40] T. Head,[41] T. Hebbeker,[18] D. Hedin,[47] H. Hegab,[71] A. P. Heinson,[43] U. Heintz,[72] C. Hensel,[20] I. Heredia-De La Cruz,[29] K. Herner,[58] G. Hesketh,[41,¶] M. D. Hildreth,[51] R. Hirosky,[76] T. Hoang,[44] J. D. Hobbs,[67] B. Hoeneisen,[9] M. Hohlfeld,[21] I. Howley,[73] Z. Hubacek,[7,15] V. Hynek,[7] I. Iashvili,[64] Y. Ilchenko,[74] R. Illingworth,[45] A. S. Ito,[45] S. Jabeen,[72] M. Jaffré,[13] A. Jayasinghe,[70] R. Jesik,[40] K. Johns,[42] E. Johnson,[59] M. Johnson,[45] A. Jonckheere,[45] P. Jonsson,[40] J. Joshi,[43] A. W. Jung,[45] A. Juste,[37] K. Kaadze,[54] E. Kajfasz,[12] D. Karmanov,[34] P. A. Kasper,[45] I. Katsanos,[61] R. Kehoe,[74] S. Kermiche,[12] N. Khalatyan,[45] A. Khanov,[71] A. Kharchilava,[64] Y. N. Kharzheev,[32] I. Kiselevich,[33] J. M. Kohli,[24] A. V. Kozelov,[35] J. Kraus,[60] S. Kulikov,[35] A. Kumar,[64] A. Kupco,[8] T. Kurča,[17] V. A. Kuzmin,[34] S. Lammers,[49] G. Landsberg,[72] P. Lebrun,[17] H. S. Lee,[28] S. W. Lee,[52] W. M. Lee,[45] J. Lellouch,[14] H. Li,[11] L. Li,[43] Q. Z. Li,[45] J. K. Lim,[28] D. Lincoln,[45] J. Linnemann,[59] V. V. Lipaev,[35] R. Lipton,[45] H. Liu,[74] Y. Liu,[4] A. Lobodenko,[36] M. Lokajicek,[8] R. Lopes de Sa,[67] H. J. Lubatti,[77] R. Luna-Garcia,[29,**] A. L. Lyon,[45] A. K. A. Maciel,[1] R. Madar,[15] R. Magaña-Villalba,[29] S. Malik,[61] V. L. Malyshev,[32] Y. Maravin,[54] J. Martínez-Ortega,[29] R. McCarthy,[67] C. L. McGivern,[53] M. M. Meijer,[30,31] A. Melnitchouk,[60] D. Menezes,[47] P. G. Mercadante,[3] M. Merkin,[34] A. Meyer,[18] J. Meyer,[20] F. Miconi,[16] N. K. Mondal,[26] M. Mulhearn,[76] E. Nagy,[12] M. Naimuddin,[25] M. Narain,[72] R. Nayyar,[42] H. A. Neal,[58] J. P. Negret,[5] P. Neustroev,[36] T. Nunnemann,[22] G. Obrant,[36,§§] J. Orduna,[75] N. Osman,[12] J. Osta,[51] M. Padilla,[43] A. Pal,[73] N. Parashar,[50] V. Parihar,[72] S. K. Park,[28] R. Partridge,[72,‖] N. Parua,[49] A. Patwa,[68] B. Penning,[45] M. Perfilov,[34] Y. Peters,[41] K. Petridis,[41] G. Petrillo,[66] P. Pétroff,[13] M.-A. Pleier,[68] P. L. M. Podesta-Lerma,[29,††] V. M. Podstavkov,[45] A. V. Popov,[35] M. Prewitt,[75] D. Price,[49] N. Prokopenko,[35] J. Qian,[58] A. Quadt,[20] B. Quinn,[60] M. S. Rangel,[1] K. Ranjan,[25] P. N. Ratoff,[39] I. Razumov,[35] P. Renkel,[74] I. Ripp-Baudot,[16] F. Rizatdinova,[71] M. Rominsky,[45] A. Ross,[39] C. Royon,[15] P. Rubinov,[45] R. Ruchti,[51] G. Sajot,[11] P. Salcido,[47] A. Sánchez-Hernández,[29] M. P. Sanders,[22] B. Sanghi,[45] A. S. Santos,[1,‡‡] G. Savage,[45] L. Sawyer,[55] T. Scanlon,[40] R. D. Schamberger,[67] Y. Scheglov,[36] H. Schellman,[48] S. Schlobohm,[77] C. Schwanenberger,[41] R. Schwienhorst,[59] J. Sekaric,[53] H. Severini,[70] E. Shabalina,[20] V. Shary,[15] S. Shaw,[59] A. A. Shchukin,[35] R. K. Shivpuri,[25] V. Simak,[7] P. Skubic,[70] P. Slattery,[66] D. Smirnov,[51] K. J. Smith,[64] G. R. Snow,[61] J. Snow,[69] S. Snyder,[68] S. Söldner-Rembold,[41] L. Sonnenschein,[18] K. Soustruznik,[6] J. Stark,[11] D. A. Stoyanova,[35] M. Strauss,[70] L. Stutte,[45] L. Suter,[41] P. Svoisky,[70] M. Takahashi,[41] M. Titov,[15] V. V. Tokmenin,[32] Y.-T. Tsai,[66] K. Tschann-Grimm,[67] D. Tsybychev,[67] B. Tuchming,[15] C. Tully,[63] L. Uvarov,[36] S. Uvarov,[36] S. Uzunyan,[47] R. Van Kooten,[49] W. M. van Leeuwen,[30] N. Varelas,[46] E. W. Varnes,[42] I. A. Vasilyev,[35] P. Verdier,[17] A. Y. Verkheev,[32] L. S. Vertogradov,[32] M. Verzocchi,[45] M. Vesterinen,[41] D. Vilanova,[15] P. Vokac,[7] H. D. Wahl,[44] M. H. L. S. Wang,[45] J. Warchol,[51] G. Watts,[77] M. Wayne,[51] J. Weichert,[21] L. Welty-Rieger,[48] A. White,[73] D. Wicke,[23] M. R. J. Williams,[39] G. W. Wilson,[53] M. Wobisch,[55] D. R. Wood,[57] T. R. Wyatt,[41] Y. Xie,[45] R. Yamada,[45] W.-C. Yang,[41] T. Yasuda,[45] Y. A. Yatsunenko,[32] W. Ye,[67] Z. Ye,[45] H. Yin,[45] K. Yip,[68] S. W. Youn,[45] J. Zennamo,[64] T. Zhao,[77] T. G. Zhao,[41] B. Zhou,[58] J. Zhu,[58] M. Zielinski,[66] D. Zieminska,[49] and L. Zivkovic[72]

 

(The D0 Collaboration)

[1]*LAFEX, Centro Brasileiro de Pesquisas Físicas, Rio de Janeiro, Brazil*
[2]*Universidade do Estado do Rio de Janeiro, Rio de Janeiro, Brazil*
[3]*Universidade Federal do ABC, Santo André, Brazil*
[4]*University of Science and Technology of China, Hefei, People's Republic of China*
[5]*Universidad de los Andes, Bogotá, Colombia*
[6]*Charles University, Faculty of Mathematics and Physics, Center for Particle Physics, Prague, Czech Republic*
[7]*Czech Technical University in Prague, Prague, Czech Republic*
[8]*Center for Particle Physics, Institute of Physics, Academy of Sciences of the Czech Republic, Prague, Czech Republic*
[9]*Universidad San Francisco de Quito, Quito, Ecuador*
[10]*LPC, Université Blaise Pascal, CNRS/IN2P3, Clermont, France*
[11]*LPSC, Université Joseph Fourier Grenoble 1, CNRS/IN2P3, Institut National Polytechnique de Grenoble, Grenoble, France*
[12]*CPPM, Aix-Marseille Université, CNRS/IN2P3, Marseille, France*
[13]*LAL, Université Paris-Sud, CNRS/IN2P3, Orsay, France*
[14]*LPNHE, Universités Paris VI and VII, CNRS/IN2P3, Paris, France*
[15]*CEA, Irfu, SPP, Saclay, France*
[16]*IPHC, Université de Strasbourg, CNRS/IN2P3, Strasbourg, France*
[17]*IPNL, Université Lyon 1, CNRS/IN2P3, Villeurbanne, France and Université de Lyon, Lyon, France*
[18]*III. Physikalisches Institut A, RWTH Aachen University, Aachen, Germany*
[19]*Physikalisches Institut, Universität Freiburg, Freiburg, Germany*
[20]*II. Physikalisches Institut, Georg-August-Universität Göttingen, Göttingen, Germany*
[21]*Institut für Physik, Universität Mainz, Mainz, Germany*
[22]*Ludwig-Maximilians-Universität München, München, Germany*
[23]*Fachbereich Physik, Bergische Universität Wuppertal, Wuppertal, Germany*
[24]*Panjab University, Chandigarh, India*
[25]*Delhi University, Delhi, India*
[26]*Tata Institute of Fundamental Research, Mumbai, India*
[27]*University College Dublin, Dublin, Ireland*
[28]*Korea Detector Laboratory, Korea University, Seoul, Korea*
[29]*CINVESTAV, Mexico City, Mexico*
[30]*Nikhef, Science Park, Amsterdam, the Netherlands*
[31]*Radboud University Nijmegen, Nijmegen, the Netherlands*
[32]*Joint Institute for Nuclear Research, Dubna, Russia*
[33]*Institute for Theoretical and Experimental Physics, Moscow, Russia*
[34]*Moscow State University, Moscow, Russia*
[35]*Institute for High Energy Physics, Protvino, Russia*
[36]*Petersburg Nuclear Physics Institute, St. Petersburg, Russia*
[37]*Institució Catalana de Recerca i Estudis Avançats (ICREA) and Institut de Física d'Altes Energies (IFAE), Barcelona, Spain*
[38]*Uppsala University, Uppsala, Sweden*
[39]*Lancaster University, Lancaster LA1 4YB, United Kingdom*
[40]*Imperial College London, London SW7 2AZ, United Kingdom*
[41]*The University of Manchester, Manchester M13 9PL, United Kingdom*
[42]*University of Arizona, Tucson, Arizona 85721, USA*
[43]*University of California Riverside, Riverside, California 92521, USA*
[44]*Florida State University, Tallahassee, Florida 32306, USA*
[45]*Fermi National Accelerator Laboratory, Batavia, Illinois 60510, USA*
[46]*University of Illinois at Chicago, Chicago, Illinois 60607, USA*
[47]*Northern Illinois University, DeKalb, Illinois 60115, USA*
[48]*Northwestern University, Evanston, Illinois 60208, USA*
[49]*Indiana University, Bloomington, Indiana 47405, USA*
[50]*Purdue University Calumet, Hammond, Indiana 46323, USA*
[51]*University of Notre Dame, Notre Dame, Indiana 46556, USA*
[52]*Iowa State University, Ames, Iowa 50011, USA*
[53]*University of Kansas, Lawrence, Kansas 66045, USA*
[54]*Kansas State University, Manhattan, Kansas 66506, USA*
[55]*Louisiana Tech University, Ruston, Louisiana 71272, USA*
[56]*Boston University, Boston, Massachusetts 02215, USA*
[57]*Northeastern University, Boston, Massachusetts 02115, USA*

[58]University of Michigan, Ann Arbor, Michigan 48109, USA
[59]Michigan State University, East Lansing, Michigan 48824, USA
[60]University of Mississippi, University, Mississippi 38677, USA
[61]University of Nebraska, Lincoln, Nebraska 68588, USA
[62]Rutgers University, Piscataway, New Jersey 08855, USA
[63]Princeton University, Princeton, New Jersey 08544, USA
[64]State University of New York, Buffalo, New York 14260, USA
[65]Columbia University, New York, New York 10027, USA
[66]University of Rochester, Rochester, New York 14627, USA
[67]State University of New York, Stony Brook, New York 11794, USA
[68]Brookhaven National Laboratory, Upton, New York 11973, USA
[69]Langston University, Langston, Oklahoma 73050, USA
[70]University of Oklahoma, Norman, Oklahoma 73019, USA
[71]Oklahoma State University, Stillwater, Oklahoma 74078, USA
[72]Brown University, Providence, Rhode Island 02912, USA
[73]University of Texas, Arlington, Texas 76019, USA
[74]Southern Methodist University, Dallas, Texas 75275, USA
[75]Rice University, Houston, Texas 77005, USA
[76]University of Virginia, Charlottesville, Virginia 22901, USA
[77]University of Washington, Seattle, Washington 98195, USA

(Received 26 April 2012; published 26 November 2012)

We investigate the decay $B_s^0 \to J/\psi K^+K^-$ for invariant masses of the $K^+K^-$ pair in the range $1.35 < M(K^+K^-) < 2$ GeV. The data sample corresponds to an integrated luminosity of 10.4 fb$^{-1}$ of $p\bar{p}$ collisions at $\sqrt{s} = 1.96$ TeV accumulated with the D0 detector at the Fermilab Tevatron collider. From the study of the invariant mass and spin of the $K^+K^-$ system, we find evidence for the two-body decay $B_s^0 \to J/\psi f_2'(1525)$ and measure the relative branching fraction of the decays $B_s^0 \to J/\psi f_2'(1525)$ and $B_s^0 \to J/\psi\phi$ to be $R_{f_2'/\phi} = 0.19 \pm 0.05(\text{stat}) \pm 0.04(\text{syst})$.

DOI: 10.1103/PhysRevD.86.092011 PACS numbers: 13.25.Hw, 14.20.Gk

## I. INTRODUCTION

In the standard model [1], the mixing of quarks originates from their interactions with the Higgs field causing the quark mass eigenstates to be different from the quark flavor eigenstates. Constraints on the mixing phases are obtained from measurements of the decays of neutral mesons. Decays to final states that are common to both partners of a neutral-meson doublet are of particular importance. The interference between the amplitude of the direct decay and the amplitude of the decay following the particle-antiparticle oscillation may lead to a $CP$-violating asymmetry between decays of mesons and antimesons. The decays $B_s^0 \to J/\psi X$, where $X$ stands for a pair of charged kaons or pions, are a sensitive probe for new phenomena because the $CP$-violating phase that appears in such decays is predicted in the standard model to be close to zero with high precision [2].

The first observation of the decay sequence $B_s^0 \to J/\psi f_2'(1525)$, $f_2'(1525) \to K^+K^-$, was recently reported by LHCb [3]. The spin $J = 2$ assignment for the $K^+K^-$ pair was based on excluding pure $J = 0$. In this article, we confirm the presence of the decay $B_s^0 \to J/\psi K^+K^-$ with $K^+K^-$ invariant masses $M(K^+K^-)$ close to 1.52 GeV and we determine that the spin of the $K^+K^-$ resonance is consistent with $J = 2$ and is preferred over $J = 0$ or $J = 1$ assignments. We identify the resonance as the $f_2'(1525)$ meson and measure the branching fraction relative to the well established decay $B_s^0 \to J/\psi\phi$.

## II. DETECTOR

The D0 detector consists of a central tracking system, a calorimetry system and muon detectors, as detailed in Refs. [4–6]. The central tracking system comprises a silicon microstrip tracker (SMT) and a central fiber tracker, both located inside a 1.9 T superconducting solenoidal magnet. The tracking system is designed to optimize tracking and vertexing for pseudorapidities $|\eta| < 3$, where

[*]Visitor from Augustana College, Sioux Falls, SD, USA.
[†]Visitor from The University of Liverpool, Liverpool, UK.
[‡]Visitor from UPIITA-IPN, Mexico City, Mexico.
[§]Visitor from DESY, Hamburg, Germany.
[‖]Visitor from SLAC, Menlo Park, CA, USA.
[¶]Visitor from University College London, London, UK.
[**]Visitor from Centro de Investigacion en Computacion-IPN, Mexico City, Mexico.
[††]Visitor from ECFM, Universidad Autonoma de Sinaloa, Culiacán, Mexico.
[‡‡]Visitor from Universidade Estadual Paulista, São Paulo, Brazil.
[§§]Deceased.

$\eta = -\ln[\tan(\theta/2)]$ and $\theta$ is the polar angle with respect to the proton beam direction.

The SMT can reconstruct the $p\bar{p}$ interaction vertex (PV) for interactions with at least three tracks with a precision of 40 $\mu$m in the plane transverse to the beam direction and determine the impact parameter of any track relative to the PV with a precision between 20 and 50 $\mu$m, depending on the number of hits in the SMT.

The muon detector surrounds the calorimeter. It consists of a central muon system covering the pseudorapidity region $|\eta| < 1$ and a forward muon system covering the pseudorapidity region $1 < |\eta| < 2$. Both systems consist of a layer of drift tubes and scintillators inside 1.8 T toroidal magnets and two similar layers outside the toroids.

## III. EVENT RECONSTRUCTION AND CANDIDATE SELECTION

The analysis presented here is based on a data sample corresponding to an integrated luminosity of 10.4 fb$^{-1}$ accumulated between February 2002 and September 2011 at the Fermilab Tevatron collider. Events are collected with single-muon and dimuon triggers. Some triggers require the presence of tracks with a large impact parameter with respect to the PV. The events selected exclusively by these triggers are removed from our sample.

Candidate $B_s^0 \to J/\psi K^+K^-$, $J/\psi \to \mu^+\mu^-$ events are required to include two oppositely charged muons accompanied by two oppositely charged tracks. Both muons are required to be detected in the muon chambers inside the toroidal magnet, and at least one of the muons is required to be also detected outside the toroid. Each of the four tracks is required to have at least one SMT hit. In addition, the kaon candidates are required to have at least two hits in the SMT, at least two hits in the central fiber tracker, and a total of at least eight hits in both detectors.

To form $B_s^0$ candidates, muon pairs in the invariant mass range $2.9 < M(\mu^+\mu^-) < 3.3$ GeV, consistent with $J/\psi$ decay, are combined with pairs of oppositely charged particles (assigned the kaon mass), consistent with production at a common vertex. A kinematic fit under the $B_s^0$ decay hypothesis constrains $M(\mu^+\mu^-)$ to the Particle Data Group [1] value of the $J/\psi$ mass and the four tracks to a common vertex. The trajectories of the four $B_s^0$ decay products are adjusted according to this kinematic fit. In events where multiple candidates satisfy these requirements, we select the candidate with the best fit probability. The $\chi^2$ of the fit is required to be less than 15, for a total number of degrees of freedom of 4. We require that the transverse momenta of the $B_s^0$ and $K^\pm$ mesons are larger than 8 and 0.7 GeV, respectively. To suppress background from the decay $B^0 \to J/\psi K^*(892)$, we require the kaon pair to have an invariant mass greater than 1 GeV under the $K^\pm\pi^\mp$ hypothesis.

To reconstruct the PV, we select tracks that do not originate from the candidate $B_s^0$ decay and apply a constraint to the average beam-spot position [4] in the transverse plane. We define the signed decay length of a $B_s^0$ meson, $L_{xy}^B$, as the vector pointing from the PV to the decay vertex, projected on the $B_s^0$ transverse momentum $p_T$. The proper decay time of a $B_s^0$ candidate is given by $t = M_{B_s}\vec{L}_{xy}^B \cdot \vec{p}/(p_T^2)$ where $M_{B_s}$ is the world-average $B_s^0$ mass [1] and $\vec{p}$ is the particle momentum. To increase $B_s^0$ signal purity and reject prompt background, we require the proper decay length to be greater than 200 $\mu$m. The distribution of the uncertainty on the proper decay length peaks around 25 $\mu$m and has a long tail extending to several hundred microns. To remove poorly reconstructed events in the tail, we require the uncertainty of the proper decay length to be less than 100 $\mu$m.

## IV. MONTE CARLO SAMPLES

Some aspects of this analysis require information that cannot be derived from data. We rely on Monte Carlo (MC) simulated samples to derive templates of the distributions of the signal $B_s^0 \to J/\psi f_2'(1525)$ and of the main background components, and to derive the detector acceptance as a function of decay angles and the relative acceptance for the decays $B_s^0 \to J/\psi\phi$ and $B_s^0 \to J/\psi f_2'(1525)$.

We use PYTHIA [7] to generate $B_s^0$ mesons and EVTGEN [8] to simulate their decay. In all simulated samples the final states are assumed to have no polarization. The samples have been processed by the detector simulation and the standard event reconstruction. To take into account the effects of the instantaneous luminosity, the MC samples are overlaid with data events collected during random beam crossings. We have generated events containing the decays $B_s^0 \to J/\psi f_2'(1525)$, $B_s^0 \to J/\psi\phi$, $B^0 \to J/\psi K_2^*(1430)$, and $B^0 \to J/\psi K_0^*(1430)$.

## V. $B_s^0 \to J/\psi K^+K^-$ SIGNAL EXTRACTION

The distribution of the $B_s^0$ candidate mass $M(J/\psi K^+K^-)$ as a function of $M(K^+K^-)$ for accepted events is shown in Fig. 1. The data show a structure consistent with the decay $B_s^0 \to J/\psi f_2'(1525)$. Another possibility for the observed structure near $M(K^+K^-) = 1.5$ GeV is the decay $B_s^0 \to J/\psi f_0(1500)$. The two states have very different branching fractions to $\pi^+\pi^-$ and $K^+K^-$. The branching fractions [1] are $\mathcal{B}(f_0(1500) \to \pi\pi) = (34.9 \pm 2.3)\%$, $\mathcal{B}(f_0(1500) \to K\bar{K}) = (8.6 \pm 1.0)\%$, $\mathcal{B}(f_2'(1525) \to \pi\pi) = (0.82 \pm 0.15)\%$, and $\mathcal{B}(f_2'(1525) \to K\bar{K} = (88.7 \pm 2.2)\%$. If the $M(K^+K^-)$ peak is due to the $f_0(1500)$, a larger peak is expected near $M(\pi^+\pi^-) = 1.5$ GeV. If the $M(K^+K^-)$ peak is due to the $f_2'(1525)$ meson, a negligibly small peak is expected in the $M(\pi^+\pi^-)$ distribution. From the lack of significant $B_s^0$ signal in the $\pi^+\pi^-$ channel, presented in Fig. 2, we conclude that the observed state is not the $f_0(1500)$ meson.

However, as observed by others [3,9], a similar distribution may also result from decays of $B^0$ mesons where the

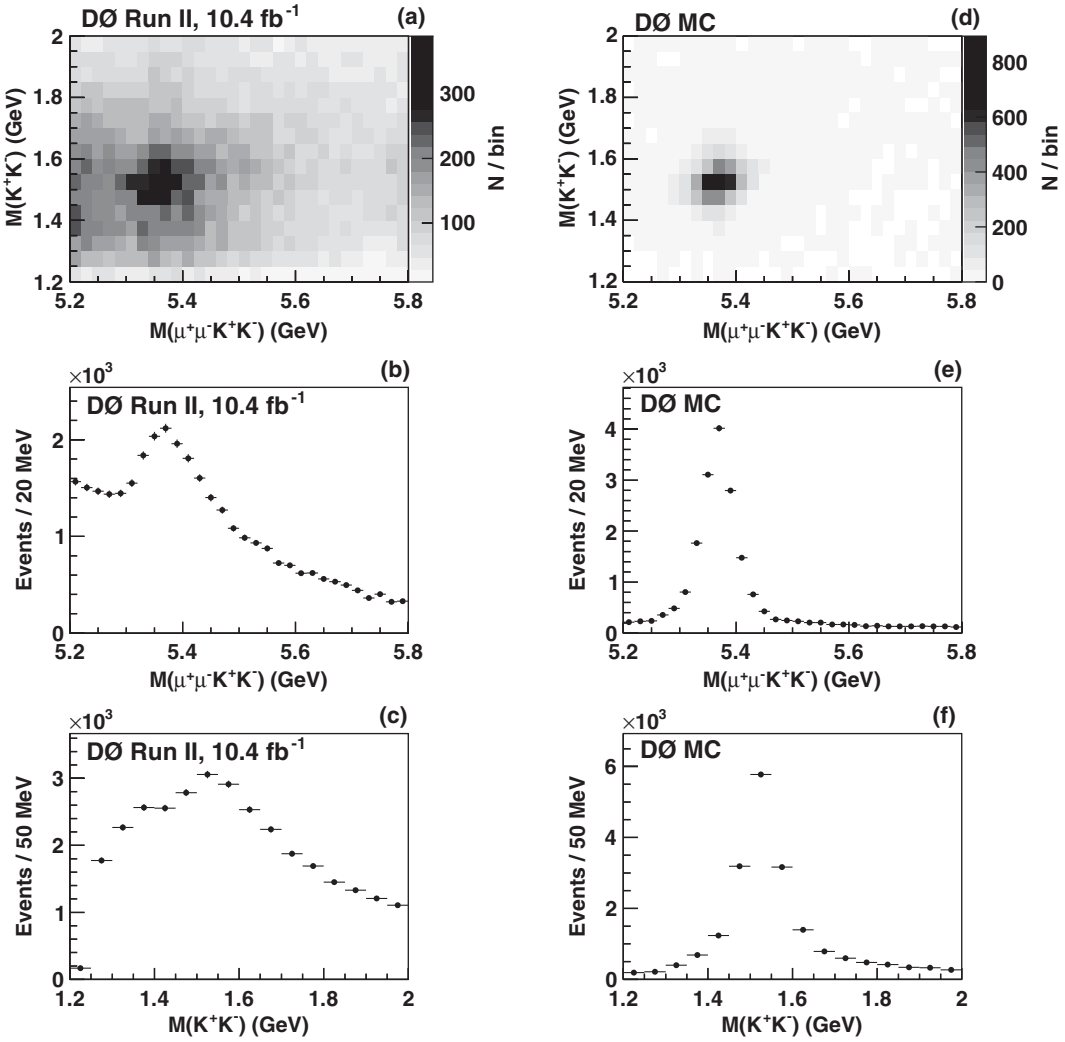


FIG. 1. (a) Invariant mass of the $B_s^0$ candidates as a function of $M(K^+K^-)$ as well as (b) and (c) one-dimensional projections. The observed structure is consistent with a decay $B_s^0 \to J/\psi K^+K^-$ proceeding through $f_2'(1525)$ or $f_0(1500)$ mesons. (d) Invariant mass of the $B_s^0$ mesons as a function of $M(K^+K^-)$ for the simulated decay $B_s^0 \to J/\psi f_2'(1525)$ as well as (e) and (f) one-dimensional projections.

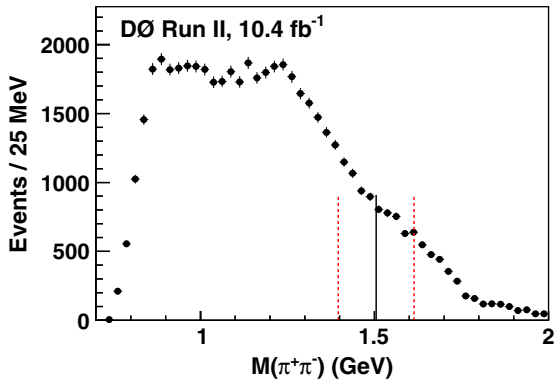


FIG. 2 (color online). Distribution of the invariant mass $M(\pi^+\pi^-)$. The solid and dashed vertical lines represent the world-average mass and the natural width of the $f_0(1500)$ meson [1], respectively.

$J/\psi$ meson is accompanied by a $K^*$ resonance, and a pion from the decay $K^* \to K^\pm\pi^\mp$ is assigned the kaon mass.

There are two $K_J^*(1430)$ states, degenerate in mass but differing in width, $\Gamma = 0.109 \pm 0.005$ GeV for $J = 2$ and $\Gamma = 0.27 \pm 0.08$ GeV for $J = 0$ [1]. Simulated distributions of $B_s^0$ mass versus $M(K^+K^-)$ for misidentified decays $B^0 \to J/\psi K_2^*(1430)$ and $B^0 \to J/\psi K_0^*(1430)$ are shown in Fig. 3. In the case of $J = 0$, we use the full $I = 1/2$ $K\pi$ elastic scattering $\mathcal{S}$-wave amplitude [9] composed of $K_0^*(1430)$ and a nonresonant term.

As seen in Fig. 3, the decays $B^0 \to J/\psi K_J^*(1430)$ with $J = 0, 2$ can mimic the decay $B_s^0 \to J/\psi f_2'(1525)$, with the apparent $B_s^0$ mass peak position increasing with $M(K^+K^-)$. We take this peaking background into account by constructing templates of the $B_s^0$ mass distribution in steps of the $K^+K^-$ invariant mass of 50 MeV. Examples of the templates are shown in Figs. 4 and 5. Figure 6 shows the

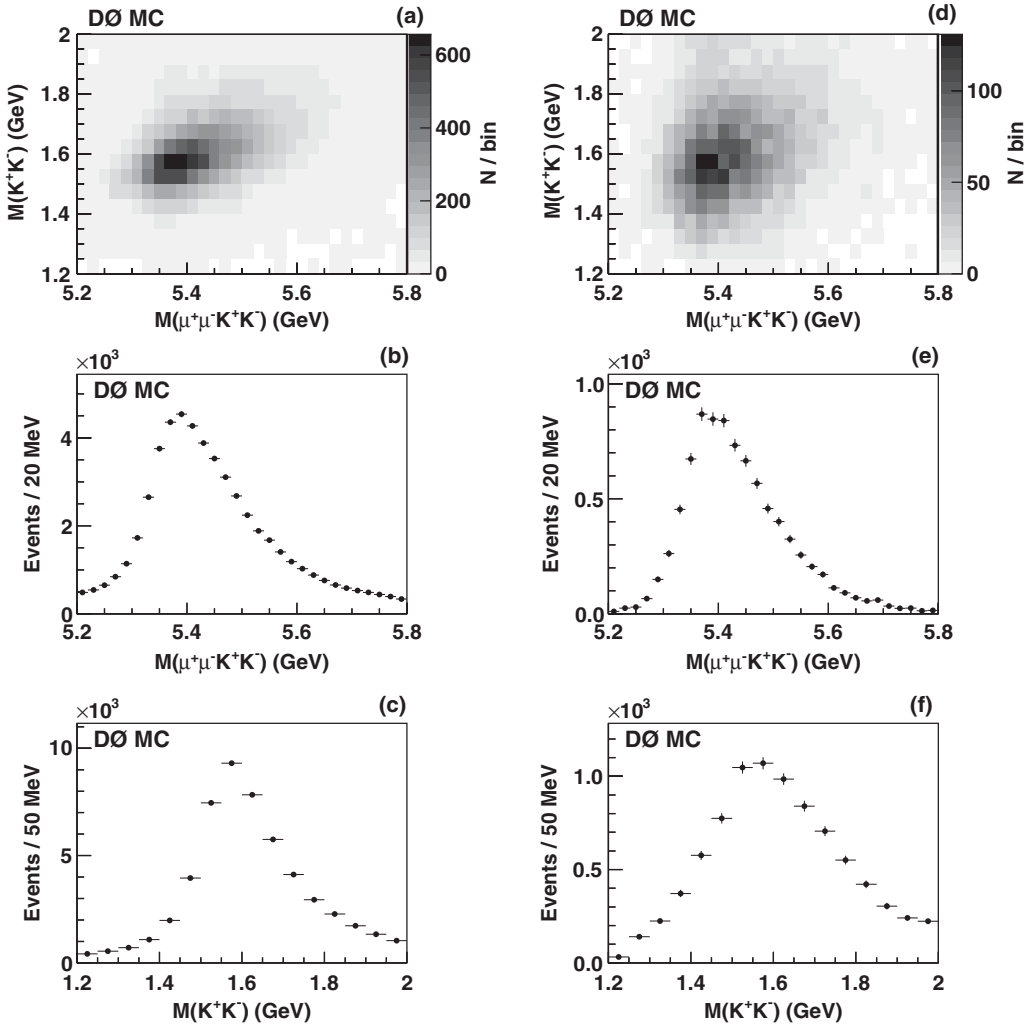


FIG. 3. (a) Invariant mass of the $B_s^0$ candidates versus $M(K^+K^-)$ for simulated decay $B^0 \to J/\psi K_2^*(1430)$; $K_2^* \to \pi^\pm K^\mp$, with the pion assigned the kaon mass, as well as (b) and (c) one-dimensional projections. (d) $K\pi$ $\mathcal{S}$-wave contribution [9] to the decay $B^0 \to J/\psi K^\pm \pi^\mp$, with the pion assigned the kaon mass as well as (e) and (f) one-dimensional projections.

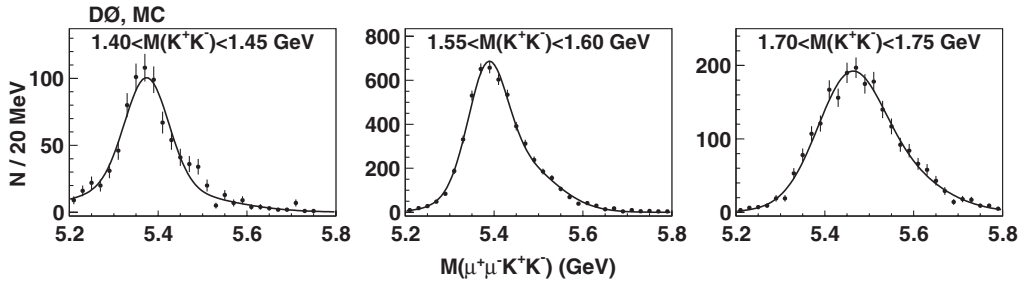


FIG. 4. Invariant mass of $B^0$ mesons from the simulated decay $B^0 \to J/\psi K_2^*(1430)$, $K_2^*(1430) \to K^\pm \pi^\mp$, where the pion is assigned the kaon mass, for a sampling of different $M(K^+K^-)$ ranges. The distributions are fitted with a sum of two Gaussian functions with free masses, widths, and normalizations.

simulated $B_s^0 \to J/\psi f_2'(1525)$ signal in the same $M(K^+K^-)$ ranges, with fits to a sum of two Gaussian functions.

Other possible sources of peaking background include $B$-meson decays to $J/\psi$ mesons accompanied by the $J = 1$ and $J = 3$ resonances $K^*(1410)$ and $K_3^*(1780)$. The former decays predominantly to $K^*(892)$. When the kaon mass is used for both tracks, the latter resonance would peak at $M(K^+K^-)$ greater than 1.78 GeV.

The candidate mass distribution in the range $1.45 < M(K^+K^-) < 1.60$ GeV and $|\cos\psi| < 0.8$ is shown in Fig. 7, where $\psi$ is the helicity angle defined in Sec. VI.

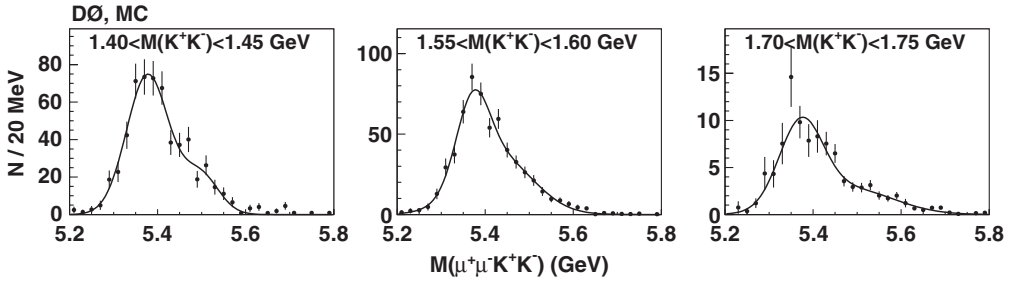


FIG. 5. Invariant mass of $B^0$ mesons from the simulated $K\pi$ $\mathcal{S}$-wave contribution [9] to the decay $B^0 \to J/\psi K^{\pm}\pi^{\mp}$, where the pion is assigned the kaon mass, for a sampling of different $M(K^+K^-)$ ranges. The distributions are fitted with a sum of two Gaussian functions with free masses, widths, and relative normalizations.

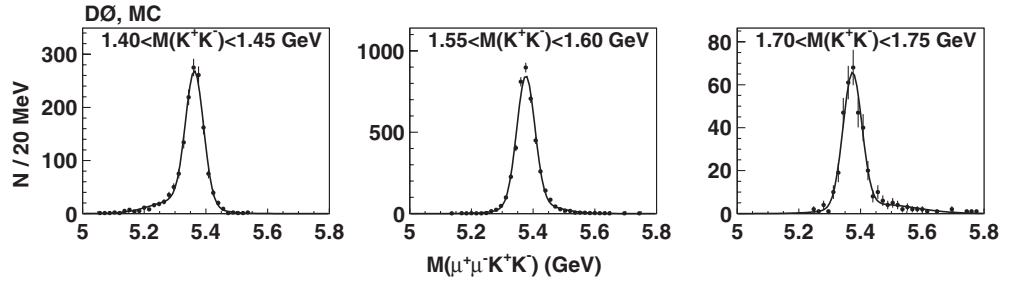


FIG. 6. Invariant mass of $B_s^0$ mesons from the simulated decay $B_s^0 \to J/\psi f_2'(1525)$ for a sampling of different ranges of $M(K^+K^-)$. The distributions are fitted with a sum of two Gaussian functions with free masses, widths, and relative normalization.

A fit of templates for the $B_s^0 \to J/\psi K^+K^-$ decay, the $B^0 \to J/\psi K_2^*(1430)$ and $\mathcal{S}$-wave $K\pi$ background and a linear combinatorial background, yields $534 \pm 101$ $B_s^0 \to J/\psi K^+K^-$ events. The relative rate of the $\mathcal{S}$ and $\mathcal{D}$ $K\pi$ wave is constrained to the ratio of 3:2 reported in Ref. [9].

To extract the $B_s^0$ signal yield, we use the $B_s^0$ mass distribution for $M(K^+K^-)$ between 1.35 and 2 GeV. We fit the simulated signal templates to the data, with the mass parameter of the core Gaussian function in each $M(K^+K^-)$ bin scaled by a factor of $0.9982 \pm 0.0008$ obtained by matching the simulation and data as shown in Fig. 7. Figure 8 shows the $B_s^0$ mass fits using the templates for the signal $B_s^0 \to J/\psi f_2'(1525)$ and for the $B^0 \to J/\psi K_2^*(1430)$ and $B^0 \to J/\psi K_0^*(1430)$ reflections. In these fits we allow the relative rates of the $\mathcal{S}$ and $\mathcal{D}$ $K\pi$ contributions to vary. Note that a nonresonant $K^+K^-$ component is implicitly included in the signal part of these fits. In addition to the peaking background there is a background due to random combinations and partially reconstructed $B$-meson decays, described by a linear function. We allow the relative normalization of the two $K_J^*$ states to vary in each fit. The normalization parameters of the $B_s^0$ signal and background components are not constrained to be positive in order to obtain unbiased results for rates close to zero. We have conducted toy MC ensemble tests and we confirm that there are no biases on signal yield introduced by the described fitting procedure.

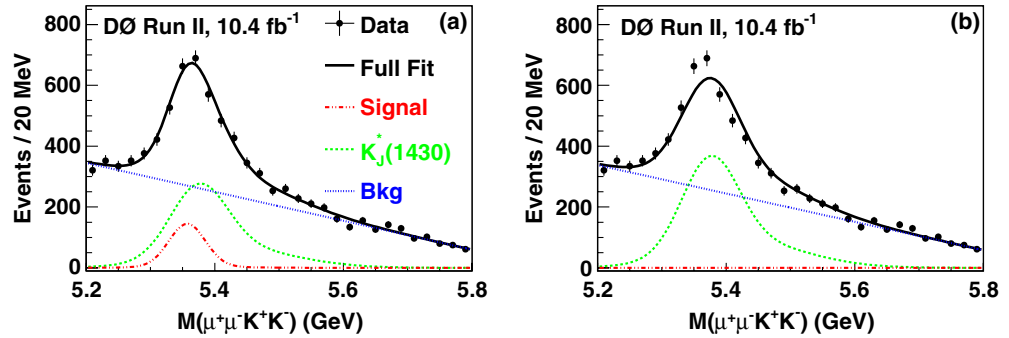


FIG. 7 (color online). Invariant mass of the $B_s^0$ candidates with $1.45 < M(K^+K^-) < 1.6$ GeV. Curves show (a) the result of the fit allowing for a free $B_s^0$ signal yield (dashed-dotted lines) and a background composed of a 3:2 mixture of $B^0 \to J/\psi K^{\pm}\pi^{\mp}$ decays with the $K^{\pm}\pi^{\mp}$ system in the $J = 0$ and $J = 2$ states (dashed lines) and a combinatorial component described by a linear function (dotted lines), and (b) the result of the fit assuming the same background model but setting the $B_s^0$ signal rate to zero.

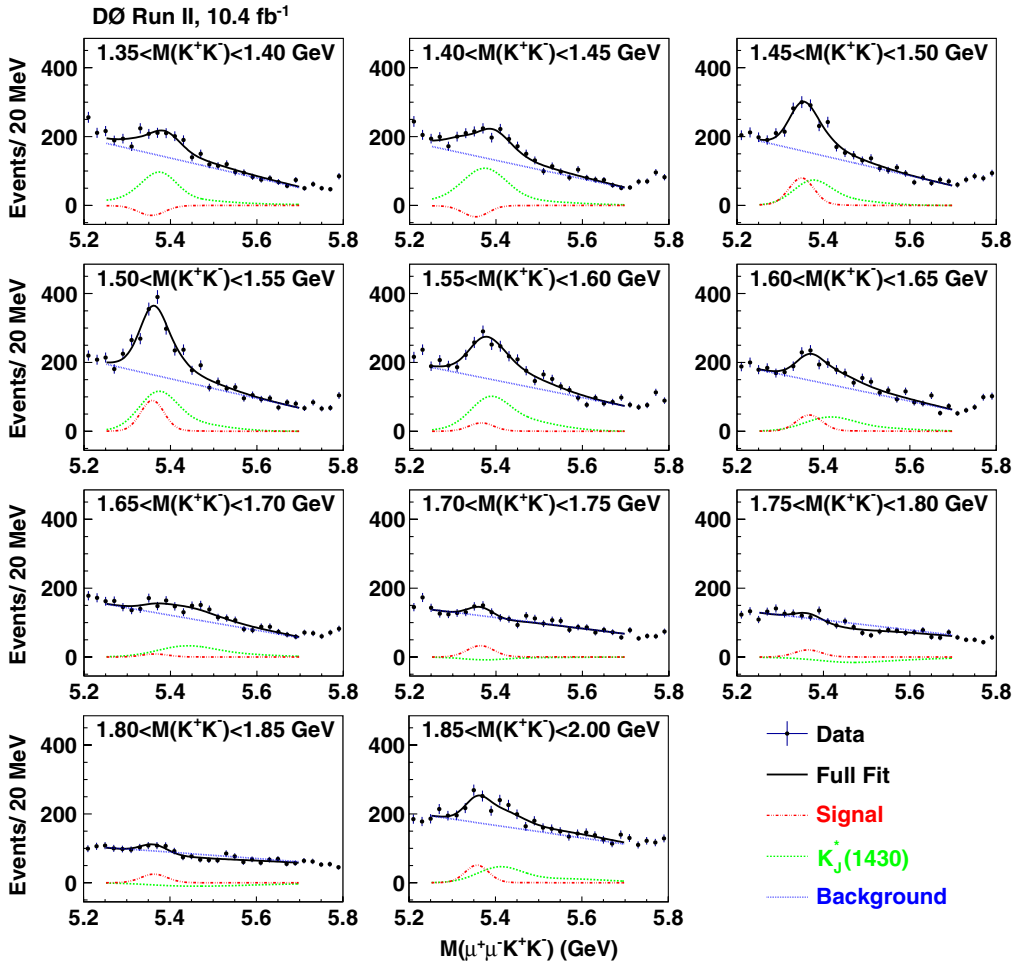


FIG. 8 (color online). Invariant mass of candidates for the decay $B_s^0 \to J/\psi K^+K^-$ in a sampling of different $M(K^+K^-)$ ranges. Each fit uses a template derived from the $B_s^0$ signal simulation, a combination of the templates for the decays $B^0 \to J/\psi K_J^*(1430)$, $K_J^*(1430) \to K^\pm\pi^\mp$, $J = 1, 2$, as shown in Figs. 4 and 5, and a linear function describing the combinatorial background. The fit is performed in the range $5.25 < M(J/\psi K^+K^-) < 5.7$ GeV, used to avoid the steeply falling background from multibody decays of $B$ mesons at lower masses and the steeply rising background from decays $B^\pm \to J/\psi K^\pm$ at higher masses. Neither the $B_s^0$ signal nor background components are constrained to positive values in order to obtain unbiased results for rates close to zero.

As seen from Fig. 8, the fitted yields for the $B^0 \to J/\psi K_2^*(1430)$ and $B^0 \to J/\psi K_0^*(1430)$ decays exceed the $B_s^0$ signal in most of the 11 subsamples, although the data do not provide a significant constraint on their relative strength. For an independent study of this background, we select events in the range $5.4 < M(J/\psi K^+K^-) < 5.6$ GeV, where the $B^0 \to J/\psi K_J^*(1430)$ decays dominate over the $B_s^0$ signal. In Fig. 9 we show the $M(K^\pm\pi^\mp)$ distribution for these events. A fit of a relativistic Breit-Wigner $J = 2$ resonance at a fixed mass of 1.43 GeV and with a floating width, over a background described by a second-order polynomial function, yields $3386 \pm 390$ $K^*(1430)$ resonance events. This is in agreement with the total number of events ascribed to the $K^*(1430)$ reflection in this mass range. The best fit result for the width is $\Gamma = 0.162 \pm 0.019$ GeV that is in between the widths of the $J = 2$ and $J = 0$ states. This study shows that we cannot establish the dominance of one background

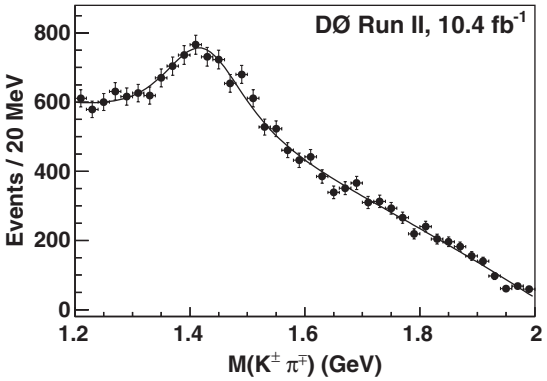


FIG. 9. Invariant mass distribution of the meson pair from the $B_s^0$ candidates in the mass range $5.4 < M(J/\psi K^+K^-) < 5.6$ GeV, under the $K^\pm\pi^\mp$ hypothesis. The curve shows the fit of a relativistic Breit-Wigner $J = 2$ resonance at a fixed mass of 1.43 GeV and with a floating width, over a background described by a second-order polynomial function.

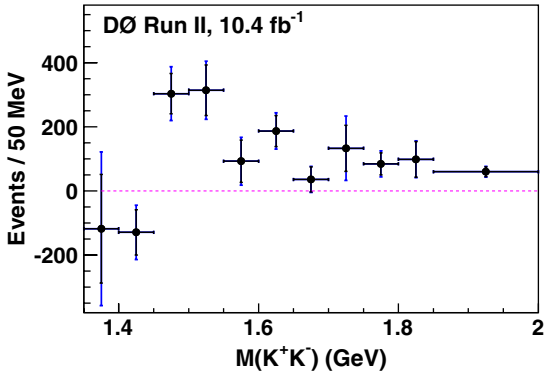


FIG. 10 (color online). The $B_s^0$ signal yield as a function of $M(K^+K^-)$ obtained from the fits shown in Fig. 8. The outer and inner error bars correspond to the statistical uncertainties with and without systematic uncertainties added in quadrature.

component over the other with the present data. Figure 10 shows the $B_s^0$ signal yield versus $M(K^+K^-)$ from data after taking into account the $B^0 \to J/\psi K_2^*(1430)$ and $B^0 \to J/\psi K_0^*(1430)$ templates and a linear background.

## VI. SPIN OF $K^+K^-$ STATE

In Sec. V, we have presented evidence for the decay $B_s^0 \to J/\psi K^+K^-$ in the range $M(K^+K^-) > 1.35$ GeV. The $M(K^+K^-)$ distribution peaks near 1.5 GeV. In this section we study the spin of the $K^+K^-$ system in the range $1.45 < M(K^+K^-) < 1.60$ GeV.

A $K^+K^-$ system can be in any natural parity state, $J^P = 0^+, 1^-, 2^+$, etc. We consider the values $J = 0$, 1, and 2 for the spin of the observed structure.

The final state can be described by three independent angles. We define them as follows: $\theta_H$ is the angle between the direction of $\mu^+$ and $B_s^0$ direction in the $J/\psi$ rest frame, $\psi$ is the angle of the $K^+$ meson with respect to the $B_s^0$ direction in the $K^+K^-$ rest frame, and $\phi_H$ is the angle between the two decay planes, as shown in Fig. 11. The angular distribution for the decay of a spinless meson into the spin-one meson $J/\psi$ and a meson of unknown spin $J$ can be expressed in terms of $H_1 = \cos\theta_H$, $H_2 = \cos\psi$, and $\phi_H$ as follows [10]:

$$\frac{d\Gamma}{d\Omega} \propto |\Sigma A_{Jm} Y_1^m(H_1, \phi_H) Y_J^{-m}(-H_2, 0)|^2 D(\Omega), \qquad (1)$$

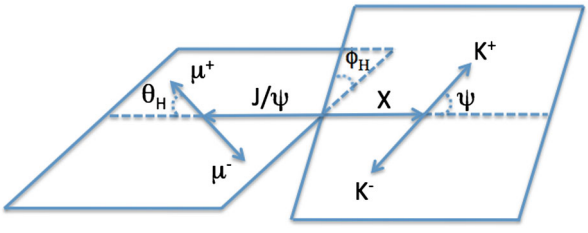


FIG. 11 (color online). Definition of the decay angles $\theta_H$, $\phi_H$, and $\psi$ in the helicity basis for the sequential decay $B_s^0 \to J/\psi X$, $J/\psi \to \mu^+\mu^-$, $X \to K^+K^-$.

where $Y_J^m$ are spherical harmonics, $A_{Jm}$ are complex amplitudes corresponding to spin $J$ and helicity $m$, and $\Omega$ is either $H_1$, $\phi_H$ or $H_2$, and the sum extends over equal helicities of the daughter particles, $m = 0$ or $m = \pm 1$. The factor $D$ is the acceptance of the event selection. Its dependence on the three angular variables is shown in Fig. 12.

Due to limited statistics and a large background, we focus on the $\cos\psi$ distribution obtained by integrating the angular distribution over $\cos\theta_H$ and $\phi_H$, taking into account the variation of the acceptance as a function of $\cos\theta_H$. We extract the $B_s^0$ signal rate as a function of $|\cos\psi|$ by fitting the candidate mass in five regions of $|\cos\psi|$. The data and fit results are shown in Fig. 13. The resulting distribution, corrected for acceptance, is shown in

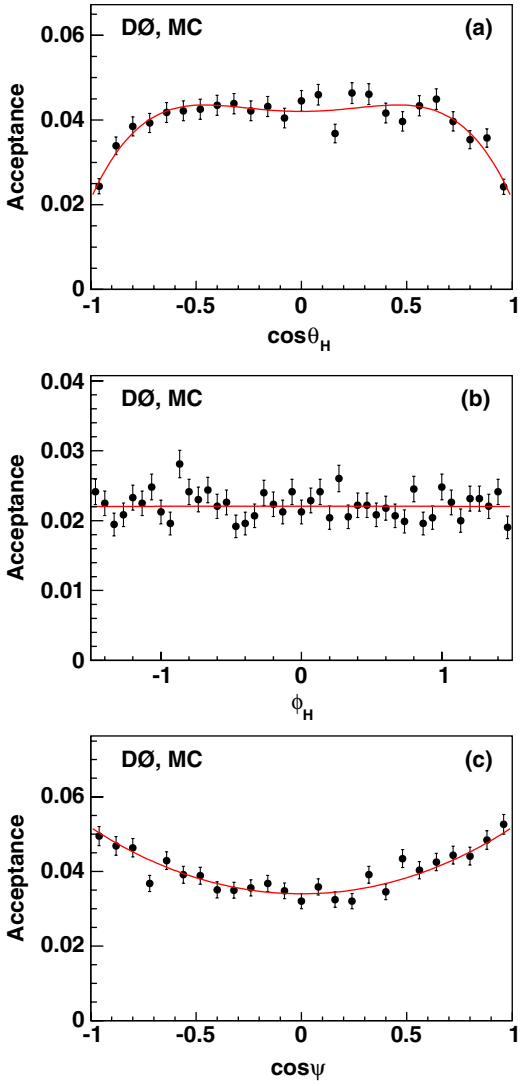


FIG. 12 (color online). Angular dependence of the detection and event selection acceptance of the decay $B_s^0 \to J/\psi f_2'(1525)$ from simulations as a function of (a) $\cos\theta_H$, (b) $\phi_H$, and (c) $\cos\psi$. The acceptance is found to be independent of the angle $\phi_H$. For $\cos\theta_H$ and $\cos\psi$, we fit the acceptance dependence with symmetric fourth-order polynomial functions.

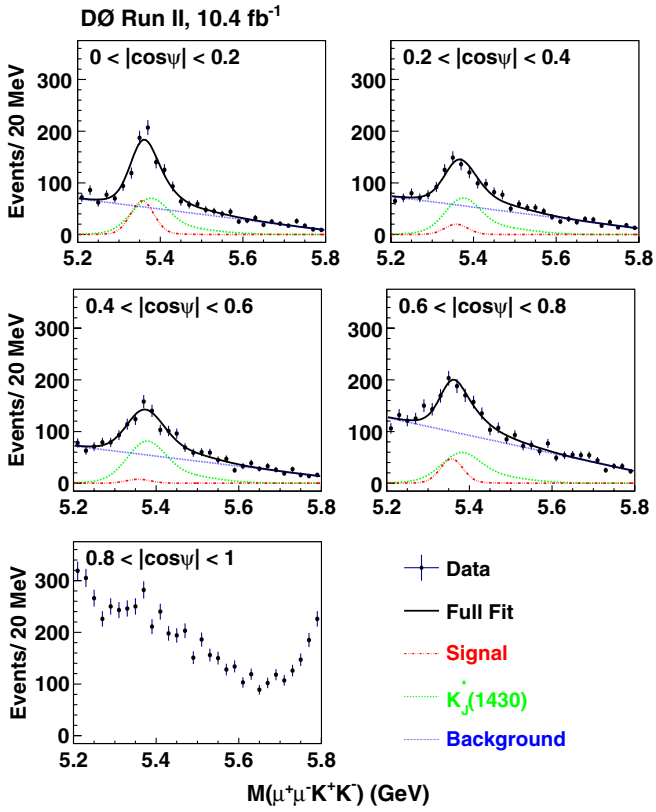


FIG. 13 (color online). The $B_s^0$ mass distribution in five intervals of $|\cos\psi|$ as shown. The fits assume a two-Gaussian $B_s^0$ signal template and a background composed of a reflection of the $B^0 \to J/\psi K^{\pm}\pi^{\mp}$ decay and a linear component. There is a steeply falling background from multibody decays of $B$ mesons at lower masses and a steeply rising background from decays $B^{\pm} \to J/\psi K^{\pm}$ at higher masses. These backgrounds are particularly acute for $\cos(\psi) > 0.8$ making it impossible to obtain a reliable fit in this region.

Fig. 14. Systematic uncertainties due to the shape of combinatorial background, signal model, and acceptance, are added in quadrature. In the region $|\cos\psi| > 0.8$, the large background prevents obtaining a reliable fit.

For $J = 0$, the expected distribution is isotropic. For $J = 1$, the $\cos\psi$ distribution without the acceptance factor is given by

$$\frac{d\Gamma}{d\cos\psi} \propto F_{10}(2\cos^2\psi) + (1 - F_{10})\sin^2\psi, \qquad (2)$$

where $F_{10}$ is the ratio of the rate $J = 1$, $m = 0$ to the total $J = 1$ rate. For a superposition of $J = 0$ and 2, with a free relative normalization, the $\cos\psi$ distribution is obtained from

$$\frac{d\Gamma}{d\cos\psi} \propto \left|\sqrt{F_{20}(1 - F_0)(5/4)}(3\cos^2\psi - 1) + \exp(i\delta_0)\sqrt{F_0}\right|^2 + \frac{15}{2}(1 - F_{20})(1 - F_0)\sin^2\psi(1 - \sin^2\psi), \qquad (3)$$

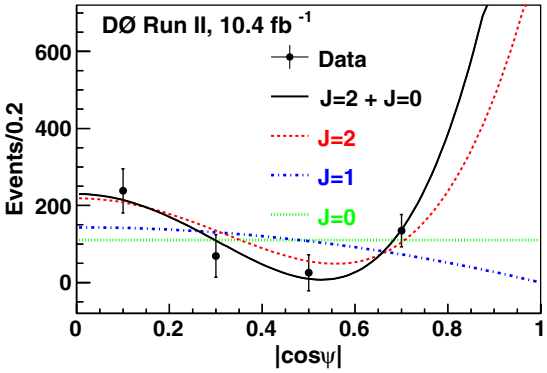


FIG. 14 (color online). The $|\cos\psi|$ distribution for the decay $B_s^0 \to J/\psi X$, $X \to K^+K^-$ in the range $1.45 < M(K^+K^-) < 1.6$ GeV. The curves are best fits assuming pure $J = 0$ (dashed line), pure $J = 1$ (dashed-dotted line), and pure $J = 2$ (solid line).

where $F_{20}$ is the ratio of the rate $J = 2$, $m = 0$ to the total $J = 2$ rate, and $F_0$ is the $J = 0$ fraction with relative phase angle $\delta_0$.

Figure 14 shows that the data favor $J = 2$, hence the peak is identified with the $f_2'(1525)$ meson. The fit probabilities for pure $J = 0$ and pure $J = 1$ are $2.8 \times 10^{-2}$ and $9.8 \times 10^{-3}$, respectively. For $J = 2$ the fit probability is 0.27. The data are also consistent with a coherent superposition of $J = 0$ and $J = 2$ states. With $F_{20} = 1$, we obtain the $\mathcal{S}$-wave fraction of $F_0 = 0.06 \pm 0.16$ and a fit probability of 0.37.

## VII. SIGNAL YIELD

The measured decay rate of a particle resonance as a function of the invariant mass of the final state is described by the relativistic Breit-Wigner function (RBW) [1] convoluted with detector resolution.

To obtain the detector resolution, we use simulated $B_s^0 \to J/\psi f_2'(1525)$ decays where the $J/\psi$ is forced to decay into two muons and the $f_2'(1525)$ into two kaons. The fitted $M(K^+K^-)$ distribution for the simulation is shown in Fig. 15. Fixing the mass and natural width parameters at their input values, $M = 1525$ MeV and $\Gamma_0 = 73$ MeV, and using the range parameter [1] $R = 5.0$ GeV$^{-1}$, we obtain $\sigma(M) = 22 \pm 1$ MeV.

We fit the $B_s^0$ signal yield versus $M(K^+K^-)$ from data, as shown in Fig. 10, to an incoherent sum of the $J = 2$ component and a constant continuum term. The result is shown in Fig. 16. The fit yields $629 \pm 157 f_2'(1525)$ events and $345 \pm 76$ events for the constant term in the mass range $1.4 < M(K^+K^-) < 1.7$ GeV. The fraction of the nonresonant term, assumed to be the $\mathcal{S}$ wave, in this mass range is $0.35 \pm 0.09$.

## VIII. RATIO OF $\mathcal{B}(B_s^0 \to J/\psi f_2'(1525))$ AND $\mathcal{B}(B_s^0 \to J/\psi\phi)$

To determine an absolute branching fraction for the $B_s^0 \to J/\psi f_2'(1525)$ decay, efficiencies, branching

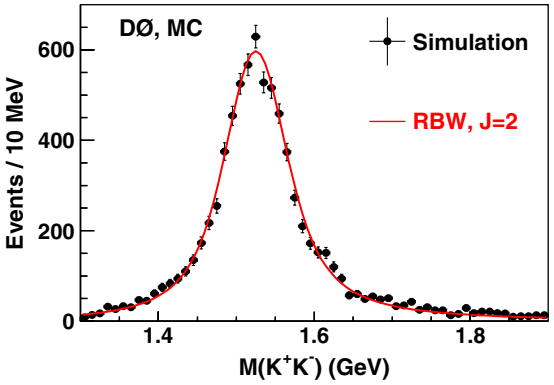


FIG. 15 (color online). The $M(K^+K^-)$ distribution from the simulation of the decay $B_s^0 \to J/\psi f_2'(1525)$ fitted by the relativistic Breit-Wigner function [1].

fractions, and the cross section need to be known, as well as the integrated luminosity. However, terms common to the $B_s^0 \to J/\psi f_2'(1525)$ and the $B_s^0 \to J/\psi\phi$ branching fractions cancel in their ratio. A measurement of the relative branching fraction $R_{f_2'/\phi}$ requires the yields of the two decays, $N_{B_s^0\to J/\psi f_2'(1525)}$ and $N_{B_s^0\to J/\psi\phi}$, and the reconstruction efficiencies of the two decay modes, $\varepsilon_{\rm reco}^{B_s^0\to J/\psi\phi}$ and $\varepsilon_{\rm reco}^{B_s^0\to J/\psi f_2'(1525)}$:

$$R_{f_2'/\phi} = \frac{\mathcal{B}(B_s^0 \to J/\psi f_2'(1525); f_2'(1525) \to K^+K^-)}{\mathcal{B}(B_s^0 \to J/\psi\phi; \phi \to K^+K^-)} = \frac{N_{B_s^0\to J/\psi f_2'(1525)} \times \varepsilon_{\rm reco}^{B_s^0\to J/\psi\phi}}{N_{B_s^0\to J/\psi\phi} \times \varepsilon_{\rm reco}^{B_s^0\to J/\psi f_2'(1525)}}, \quad (4)$$

where $N_{B_s^0\to J/\psi f_2'(1525)}$ is determined in the mass range $1.4 < M(K^+K^-) < 1.7$ GeV and $N_{B_s^0\to J/\psi\phi}$ in the mass range $1.01 < M(K^+K^-) < 1.03$ GeV. The only difference in the event selection for the two channels is the

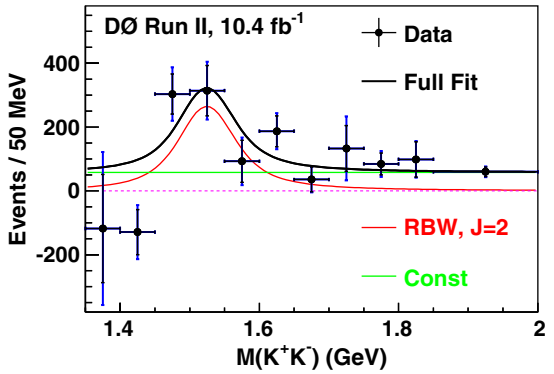


FIG. 16 (color online). Fit to the $B_s^0$ yield versus $M(K^+K^-)$ as obtained in Fig. 10. The full fit to $B_s^0 \to J/\psi K^+K^-$ includes a $f_2'(1525)$ signal described by a relativistic Breit-Wigner and nonresonant constant term for the $\mathcal{S}$ wave. The outer and inner error bars correspond to the statistical uncertainties with and without systematic uncertainties added in quadrature.

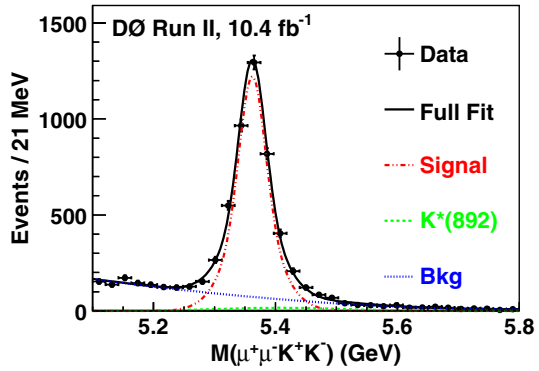


FIG. 17 (color online). Invariant mass distribution of $B_s^0$ candidates with $ct > 200$ $\mu$m for events in the mass range $1.01 < M(K^+K^-) < 1.03$ GeV. A fit to a sum of a double Gaussian $B_s^0 \to J/\psi\phi$ signal (dashed-dotted line), a quadratic combinatorial background (dotted line), and the reflection of the decay $B^0 \to J/\psi K^*(892)$ (dashed line) is used to extract the $B_s^0$ yield.

$M(K\pi) > 1$ GeV condition applied for the $J/\psi f_2'(1525)$ candidates.

The yield of the $B_s^0 \to J/\psi\phi$ decay is determined by fitting the data, shown in Fig. 17, with a double Gaussian function for the signal, a second-order polynomial for background, and the reflection of the decay $B_d^0 \to J/\psi K^*$ taken from simulations. The total number of $B_s^0 \to J/\psi\phi$ events is $4064 \pm 105$.

We use simulated samples of the two decay processes to determine the reconstruction efficiencies. For the decay $B_s^0 \to J/\psi f_2'(1525)$ the efficiency is measured to be $(0.122 \pm 0.002)\%$ and for the decay $B_s^0 \to J/\psi\phi$ it is $(0.149 \pm 0.002)\%$ (where the uncertainties are due to MC statistics), yielding $R_{f_2'/\phi} = 0.19 \pm 0.05$(stat).

The denominator in Eq. (4) may include a contribution from the $K^+K^-$ $\mathcal{S}$ wave, and no correction is made, allowing the ratio to be recalculated for different $\mathcal{S}$-wave fraction inputs.

## IX. SYSTEMATIC UNCERTAINTIES

The main contributions to systematic uncertainties are summarized in Table I. They are evaluated as follows:

(i) $K_0^*(1430)$ *width:* We vary the $K_0^*$ width within its uncertainty of 0.08 GeV [1].

(ii) $K_0^*(1430)$ *and* $K_2^*(1430)$ *templates:* We vary the shape of the $K_0^*$ and $K_2^*$ templates by altering the widths of the dominant Gaussian component within statistical uncertainties.

(iii) *Combinatorial background shape:* As an alternative, we use a second-order polynomial to describe the combinatorial background. We also vary the fitting mass range from 5.25–5.70 to 5.2–5.8 GeV.

(iv) *Signal shape:* We vary the $B_s^0$ mass scale within its uncertainty in data of 0.08% and the width of the core Gaussian component by $\pm 10\%$.

TABLE I. Sources of systematic relative uncertainty on $R_{f_2'/\phi}$.

| Source | Uncertainty (%) |
|---|---|
| $K_0^*(1430)$ width | 5 |
| $K_0^*(1430)$ and $K_2^*(1430)$ templates | 10 |
| Combinatorial background shape | 10 |
| Signal shape | 12 |
| Trigger efficiency | 3 |
| $M(K^+K^-)$ dependence of efficiency | 2 |
| Helicity dependence of efficiency | 3 |
| $f_2'(1525)$ mass | 3 |
| $f_2'(1525)$ natural width | 1 |
| $B_s^0 \to J/\psi\phi$ signal shape | 4 |
| Total | 20 |

(v) *Trigger efficiency:* Due to the mass difference between the $f_2'(1525)$ and $\phi$ resonances, there is a small difference between average muon momenta in the two channels. Approximately 3% more $J/\psi\phi$ events have a leading muon with $p_T > 15$ GeV and about 3% more $J/\psi\phi$ events have both muons with $p_T > 3$ GeV. We therefore estimate that there is approximately a 3% difference in the fraction of events that can be accepted by the trigger between the $J/\psi\phi$ and $J/\psi f_2'(1520)$ signals. Trigger simulations confirm this estimate. We apply the 3% correction to $R_{f_2'/\phi}$ and assign an absolute 3% systematic uncertainty.

(vi) $M(K^+K^-)$ *dependence of efficiency:* The $M(K^+K^-)$ dependence of the efficiency for reconstructing the $f_2'(1520)$ resonance is obtained from a simulation. We assign a 2% uncertainty due to the statistical precision of the MC sample.

(vii) *Helicity dependence of efficiency:* The $B_s^0 \to J/\psi\phi$ signal acceptance is obtained from a MC sample generated under the assumption that the final state is not polarized, i.e., with the final state distributed uniformly in helicity angle $\cos\theta_H$. We compare this signal acceptance with distributions corresponding to pure helicity 0 and 1 and assign a systematic uncertainty equal to the difference.

(viii) $f_2'(1525)$ *mass and natural width:* The uncertainty on the mass of the $f_2'(1525)$ resonance of 5 MeV [1] leads to the uncertainty on $R_{f_2'/\phi}$ of 3%, while the uncertainty on the natural width of 6 MeV leads to the uncertainty on $R_{f_2'/\phi}$ of 0.7%.

(ix) $B_s^0 \to J/\psi\phi$ *signal shape:* The $B_s^0 \to J/\psi\phi$ signal yield is sensitive to the signal mass model because of the presence of the $B_s^0 \to J/\psi K^*(890)$ reflection that peaks near the signal. We assign the systematic uncertainty as one half of the difference between fit results for single and double Gaussian distributions for the signal mass model.

## X. SUMMARY AND DISCUSSION

We confirm the observation of the decay $B_s^0 \to J/\psi f_2'(1525)$ previously observed by the LHCb Collaboration [3] and measure the ratio of branching fractions of the decays $B_s^0 \to J/\psi f_2'(1525)$ and $B_s^0 \to J/\psi\phi$ to be $R_{f_2'/\phi} = 0.19 \pm 0.05(\text{stat}) \pm 0.04(\text{syst})$. The fit to the background-subtracted signal $B_s^0 \to J/\psi K^+K^-$, assuming an incoherent sum of the $J = 2$ resonance $f_2'(1525)$ and a constant continuum term, assigns the fraction of $0.35 \pm 0.09$ to the constant term. The fit to the helicity angle $\psi$ in the $K^+K^-$ rest frame finds the $K^+K^-$ resonance to be consistent with $J = 2$ with a fit probability of 0.27 and preferred over $J = 0$ or $J = 1$, for which the fit probabilities are $2.8 \times 10^{-2}$ and $9.8 \times 10^{-3}$, respectively.

## ACKNOWLEDGMENTS

We thank the staffs at Fermilab and collaborating institutions, and acknowledge support from the DOE and NSF (U.S.); CEA and CNRS/IN2P3 (France); MON, Rosatom, and RFBR (Russia); CNPq, FAPERJ, FAPESP, and FUNDUNESP (Brazil); DAE and DST (India); Colciencias (Colombia); CONACyT (Mexico); NRF (Korea); FOM (The Netherlands); STFC and the Royal Society (U.K.); MSMT and GACR (Czech Republic); BMBF and DFG (Germany); SFI (Ireland); The Swedish Research Council (Sweden); and CAS and CNSF (China).

[1] K. Nakamura *et al.* (Particle Data Group), J. Phys. G **37**, 075021 (2010).
[2] J. Charles *et al.*, Phys. Rev. D **84**, 033005 (2011).
[3] R. Aaij *et al.* (LHCb Collaboration), Phys. Rev. Lett. **108**, 151801 (2012).
[4] V. M. Abazov *et al.* (D0 Collaboration), Nucl. Instrum. Methods Phys. Res., Sect. A **565**, 463 (2006).
[5] R. Angstadt *et al.*, Nucl. Instrum. Methods Phys. Res., Sect. A **622**, 298 (2010).
[6] V. M. Abazov *et al.*, Nucl. Instrum. Methods Phys. Res., Sect. A **552**, 372 (2005).
[7] T. Sjöstrand, S. Mrenna, and P. Scands, J. High Energy Phys. 05 (2006) 026.
[8] D. J. Lange, Nucl. Instrum. Methods Phys. Res., Sect. A **462**, 152 (2001).
[9] B. Aubert *et al.*, Phys. Rev. D **79**, 112001 (2009).
[10] A. Datta, Y. Gao, A. Gritsan, D. London, M. Nagashima, and A. Szynkman, Phys. Rev. D **77**, 114025 (2008).